Journal of Materials Chemistry B

PAPER

View Article Online
View Journal | View Issue

Cite this: J. Mater. Chem. B, 2018, 6, 3040

Reduction-responsive core-crosslinked hyaluronic acid-*b*-poly(trimethylene carbonate-*co*-dithiolane trimethylene carbonate) micelles: synthesis and CD44-mediated potent delivery of docetaxel to triple negative breast tumor *in vivo*†

Yaqin Zhu,‡[ab] Jian Zhang,‡[a] Fenghua Meng,[a] Liang Cheng,*[ac] Jan Feijen *[ab] and Zhiyuan Zhong *[a]

Received 11th January 2018,
Accepted 8th April 2018

DOI: 10.1039/c8tb00094h

rsc.li/materials-b

Future cancer therapy relies on the development of simple, selective and bioresponsive nanomedicines. Herein, we report that reduction-responsive core-crosslinked hyaluronic acid-*b*-poly(trimethylene carbonate-*co*-dithiolane trimethylene carbonate) micelles (HA-CCMs) can be easily synthesized and achieve efficient CD44-mediated delivery and triggered cytoplasmic release of docetaxel (DTX) to MDA-MB-231 human triple negative breast tumor *in vivo*. DTX-loaded HA-CCMs exhibited a favorable size of 85 nm, low drug leakage and glutathione-responsive DTX release. HA-CCMs were efficiently taken up by CD44-overexpressing MDA-MB-231 cells as indicated by flow cytometry. DTX-loaded HA-CCMs induced selective apoptotic activity toward MDA-MB-231 cells *in vitro*. Notably, over 7-fold longer blood circulation time and 4-fold stronger tumor accumulation were observed for DTX-loaded HA-CCMs compared to free DTX. Cy5-labeled HA-CCMs revealed deep tumor penetration at 6 h post injection. DTX-loaded HA-CCMs were shown to effectively suppress the progression of MDA-MB-231 tumor and significantly extend mice survival time. These hyaluronic acid-shelled and disulfide-crosslinked micelles with great simplicity and selectivity are highly promising for treating various CD44-overexpressing cancers.

Introduction

Micelles with a distinct core–shell structure are considered to be the most ideal nanocarrier for lipophilic anticancer drugs such as docetaxel (DTX).[1–3] Notably, most micelles have exploited poly(ethylene glycol) (PEG) as a shell.[4,5] In order to accomplish targeted therapy, cell-specific ligands are typically linked to the other end of PEG.[6–9] Moreover, to retard drug leakage in the circulation and enhance drug release at the tumor site, sophisticated chemistries have been employed to stabilize micelles and to endow stimuli-sensitivity, respectively.[10–13] These multifunctional micellar systems, though exhibiting improved therapeutic efficacy in animal studies, are highly complex and create formidable challenges for clinical translation.[3,14] In recent years, several groups reported that hyaluronic acid (HA)-functionalized nanomedicines can target CD44-expressing cancer cells *in vitro* and *in vivo*.[15–19] HA could also be used as a substitute for PEG to obtain CD44-targeted micelles and vesicles.[20–22]

Interestingly, our and other's recent work has demonstrated that disulfide-crosslinking can simultaneously address the problems of stability and drug release issues.[17,23–26] Based on a proprietary dithiolane trimethylene carbonate (DTC) monomer and with PEG as a hydrophilic polymer, we constructed a variety of biodegradable nanosystems for targeted cancer chemotherapy or gene therapy.[27–31] It has to be emphasized that nanosystems based on DTC are comparably easy to fabricate and subject to self-crosslinking.

In this paper, we report the fabrication and application of reduction-responsive and core-crosslinked HA-shelled micelles (HA-CCMs) for targeted delivery of DTX to CD44-overexpressing MDA-MB-231 human triple negative breast tumor *in vivo* (Scheme 1). Notably, the HA-CCMs are based on one single block copolymer, HA-*b*-poly(trimethylene carbonate-*co*-dithiolane

[a] Biomedical Polymers Laboratory, and Jiangsu Key Laboratory of Advanced Functional Polymer Design and Application, College of Chemistry, Chemical Engineering and Materials Science, Soochow University, Suzhou, 215123, P. R. China. E-mail: chengliang1983@suda.edu.cn, zyzhong@suda.edu.cn; Fax: +86-512-65880098; Tel: +86-512-65880098
[b] Department of Polymer Chemistry and Biomaterials, Faculty of Science and Technology, MIRA Institute for Biomedical Technology and Technical Medicine, University of Twente, P.O. Box 217, 7500 AE Enschede, The Netherlands. E-mail: j.feijen@utwente.nl
[c] Department of Pharmaceutics, College of Pharmaceutical Sciences, Soochow University, Suzhou 215123, P. R. China

† Electronic supplementary information (ESI) available. See DOI: 10.1039/c8tb00094h

‡ Y. Zhu and J. Zhang contributed equally to this work.

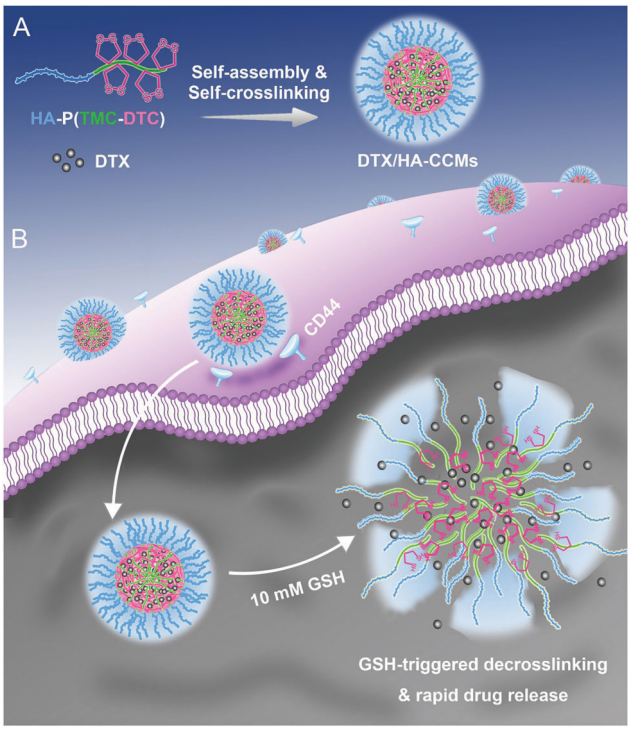

Scheme 1 Schematic illustration of reduction-responsive core-crosslinked hyaluronic acid-*b*-poly(trimethylene carbonate-*co*-dithiolane trimethylene carbonate) micelles (HA-CCMs) for CD44-mediated delivery and triggered cytoplasmic release of docetaxel (DTX) to human MDA-MB-231 triple negative breast cancer cells.

trimethylene carbonate) (HA-P(TMC-DTC)). Triple negative breast cancers (TNBCs) are difficult to treat with poor prognosis[32,33] due to their low expression level of the estrogen receptor (ER), progesteron receptor (PR), and human epidermal growth factor receptor-2 (HER2), which are often the targeting sites of antibodies or therapeutic drugs.[34,35] Here, MDA-MB-231 triple negative breast tumor was chosen as a model because it is known to overexpress CD44.[36,37] Our results revealed that DTX-loaded HA-CCMs effectively suppressed the progression of MDA-MB-231 tumor and significantly extended mice survival time. These HA-shelled and disulfide-crosslinked micelles with great simplicity and selectivity provide a promising platform for treating various CD44-overexpressing cancers.

Materials and methods

Materials

Hyaluronic acid (HA, M_w = 8 kDa, Bloomage Freda Biopharm Co., Ltd) was desalted using acidic deionized water.[38,39] Dithiolane trimethylene carbonate (DTC) was synthesized according to our previous report.[27] Free DTX (10 mg mL^{-1}) was prepared by dissolving DTX in a 1 : 1 mixture of Tween 80 and absolute ethanol. Other materials used are described in the ESI.†

Synthesis of HA-P(TMC-DTC)

The HA-P(TMC-DTC) copolymer was synthesized *via* a click reaction between HA-alkynyl (M_n = 8 kDa) and N_3-P(TMC-DTC) (M_n (^{1}H NMR) = 5.9 kDa, M_w/M_n (GPC) = 1.2), as previously reported.[40] Yield: 90%. ^{1}H NMR (600 MHz, D_2O: DMSO-d_6 = 1 : 9, Fig. S1, ESI†): HA (δ 1.80 ppm, δ 3.12–3.51 ppm and δ 4.26–4.45 ppm), TMC (δ 1.92 and 4.10 ppm), DTC (δ 3.01 and 4.10 ppm), and methine proton of triazole (δ 8.12 ppm).

Cy5-labeled HA-P(TMC-DTC) was synthesized by reacting Cy5-NH_2 with the carboxyl groups of HA. Briefly, HA-P(TMC-DTC) (50 mg, 3.6 μmol) dissolved in DMSO (1 mL) was activated with EDC (2.8 mg, 14.4 μmol) and NHS (0.8 mg, 7.2 μmol) for 15 min and then Cy5-NH_2 (3.3 mg 5.4 μmol) was added. The reaction was carried out for 24 h at 30 °C. The final product, Cy5-labeled HA-P(TMC-DTC), was isolated through extensive dialysis against DMSO for 24 h, then against DMF for 24 h followed by precipitation in cold diethyl ether and drying *in vacuo* at room temperature. Yield: 78.6%. The degree of substitution of Cy5 was 1.2 per HA chain determined by fluorescence spectrophotometry (Thermo Scientific, USA).

Preparation and characterization of blank and DTX-loaded micelles

Blank HA-CCMs were prepared by dropwise addition of the DMSO solution of HA-P(TMC-DTC) (100 μL, 10 mg mL^{-1}) to phosphate buffer (PB, 900 μL, pH 7.4, 10 mM), followed by incubation in a shaking bath overnight (37 °C, 200 rpm). Then, the micelles were extensively dialyzed against PB (10 mM, pH 7.4) for 12 h at ambient temperature. Cy5-labeled micelles were obtained by adding 10 mol% Cy5-HA-P(TMC-DTC) polymer.

DTX-loaded HA-CCMs were prepared similarly using an organic phase consisting of a mixture of HA-P(TMC-DTC) (10 mg mL^{-1} in DMSO) and DTX (10 mg mL^{-1} in DMSO). Drug loading content (DLC) and drug loading efficiency (DLE) were determined by adding an excess amount of the reductive agent DTT to DTX-loaded micelle suspensions (1 mg mL^{-1}, 200 μL) and incubating at 37 °C at 200 rpm overnight to fully de-crosslink the micelles. Subsequently, acetonitrile (800 μL) was added and incubated for 2 h to extract DTX. The solution was then filtered using a microfiltration membrane (pore size: 450 nm, Millipore, USA) and the concentration of DTX was determined with an Agilent 1260 HPLC according to our previous report.[29]

DLC and DLE were calculated using the following formulae:

$$\text{DLC (wt\%)} = (\text{weight of loaded drug/total weight of polymer and loaded drug}) \times 100$$

$$\text{DLE (\%)} = (\text{weight of loaded drug/weight of drug in feed}) \times 100$$

In vivo pharmacokinetics

The blood circulation time of DTX-loaded HA-CCMs or free DTX was evaluated by determining the DTX level in blood at different times after i.v. injection (10 mg DTX equiv. per kg). Briefly, ~50 μL of blood was taken from the retro-orbital sinus of Balb/C mice at prescribed time points. The blood samples were lysed in Triton X-100 (0.15 mL, 1%) and sonicated. To extract DTX, methanol (1 mL) was added to the blood samples and the samples were then incubated for 12 h at −20 °C.

After gentle vortexing and centrifugation at 30 065 × *g* for 15 min, the DTX concentration in the supernatant was determined by HPLC as described above. The $t_{1/2\beta}$ (elimination half-life) of DTX was calculated using the Software Origin 8.0.

In vivo imaging

Subcutaneous MDA-MB-231 human breast tumor-bearing mice were established by injecting 50 μL of MDA-MB-231 cell suspensions (2×10^8 cells per mL) into the right hind flank of mice. The experiment starts after the tumors have grown to an average volume of about 150 mm^3. To evaluate the targeting ability of HA-CCMs, 200 μL of Cy5-labeled micelles were intravenously (tail vein) injected in tumor-bearing mice at a dose of 20 mg kg^{-1}. The mice were anesthetized with pentobarbital sodium (10 mg mL^{-1} in PBS) at a dose of 62.5 mg kg^{-1} at 6, 12, 24 and 48 h post injection. Near-infrared fluorescence imaging of the mice was performed using an IVIS Lumina II imaging system (Caliper, MA, USA), Ex = 633 nm and Em = 668 nm.

Biodistribution

For the biodistribution study, MDA-MB-231 breast tumor-bearing nude mice were established as described above. Briefly, DTX-loaded HA-CCMs or free DTX (10 mg DTX equiv. per kg) was injected *via* the tail vein into the MDA-MB-231 tumor-bearing mice. After 12 h, the main organs (liver, heart, spleen, lungs and kidneys) and tumor were removed from the mice, washed with PBS and then weighed. DTX was extracted using methanol and determined by HPLC as previously reported.[29]

Tumor penetration

The tumor penetration behavior of HA-CCMs was investigated by immunofluorescence analysis. Briefly, the MDA-MB-231 breast tumor-bearing mice were tail vein injected with Cy5-labeled HA-CCMs at 20 mg kg^{-1}. Tumors were collected at 2, 6 and 12 h. After fixation in 4% formalin and embedding in paraffin, tumor blocks were sliced and stained according to our previous study.[29]

In vivo antitumor efficacy

MDA-MB-231 breast tumor bearing nude mice were established to evaluate the antitumor efficacy of DTX-loaded HA-CCMs either with a single dose or multi-dose treatment. Mice treated with PBS or free DTX were used as the control. Treatments were started when the tumor volume reached about 50 mm^3 (day 0). The mice were randomly placed in five groups (6 mice per group) and injected intravenously with the above formulations. For single dose treatment, 50 mg DTX equiv. per kg was given on day 0. Multi-dose injection was repeated every 3 days 5 times at 10 mg DTX equiv. per kg. The injection volume was 0.2 mL per 20 g of the mouse body weight. To study the active-targeting effect of HA-CCMs, one group of mice was pretreated with free HA in PBS (50 mg kg^{-1}) for 10 min before the administration of DTX-loaded HA-CCMs. Mice were weighed and tumor volumes were determined every three days using calipers according to the formula $V = 0.5 \times \text{length} \times \text{width}^2$. At day 21, the tumor and main organs of one mouse of each group were excised, fixed and sliced for hematoxylin and eosin (H&E) staining. Tumor tissues were further stained with terminal deoxynucleotidyl transferase dUTP nick end labeling (TUNEL). Finally, the stained tissues were observed with a microscope (Leica QWin, Germany).

Statistical analysis

All data are expressed as the mean ± SD. Significance among the groups was assessed by one-way analysis of variance (ANOVA), followed by *post hoc* tests (Bonferroni correction). Significance was established when $p < 0.05$.

Results and discussion

Synthesis of reduction-responsive and core-crosslinked HA-shelled micelles

The objective of this study was to create simple, selective and bioresponsive nanosystems for efficient cancer chemotherapy, for which we designed reduction-responsive core-crosslinked HA-shelled micelles (HA-CCMs). Notably, the HA-CCMs were fabricated from one single block copolymer, HA-P(TMC-DTC), in which HA serves as a hydrophilic and CD44-targeting shell whereas P(TMC-DTC) serves as a self-crosslinkable and reduction-responsive core. HA-P(TMC-DTC) was synthesized *via* a click reaction between HA-alkynyl (M_n = 8.0 kg mol^{-1}) and azido-P(TMC-DTC), which was prepared with an M_n of 5.9 kg mol^{-1} and a DTC molar fraction (F_{DTC}) of 0.15, as calculated from ^{1}H NMR (Fig. S2, ESI†). ^{1}H NMR of HA-P(TMC-DTC) (Fig. S1, ESI†) showed a peak at δ 8.12 of the methine proton of triazole. The integral ratio of peak f at δ 1.78 assignable to the methyl protons of HA and peak g (δ 8.12) was 60/1, indicating equivalent coupling between HA-alkynyl and azido-P(TMC-DTC). In addition, the FT-IR spectra (Fig. S3, ESI†) revealed that peaks at 2130 cm^{-1} (–C≡C–) of HA-alkynyl and 2100 cm^{-1} (–N=N) of N_3-P(TMC-DTC) completely disappeared, supporting the successful synthesis of HA-P(TMC-DTC).

Interestingly, HA-P(TMC-DTC) formed micelles (HA-CCMs) with a diameter of 80 nm and a low polydispersity index (PDI) of 0.07, as determined by dynamic light scattering (DLS) (Fig. 1A). TEM corroborated a uniform size distribution. As reported for HA-functionalized nanoparticles,[41,42] HA-CCMs showed a negative surface charge of −27 mV (Table 1). As anticipated, HA-CCMs are highly stable against dilution (Fig. S4A, ESI†) and 10% FBS (Fig. 1B), due to crosslinking of the micellar core *via* the spontaneous polymerization of dithiolane.[27] The self-crosslinking of disulfide bonds may be initiated by a small amount of thiols in the polymers. In addition, the ring tension of dithiolane in the micelle core may also play an important role in the cleavage of disulfide bonds. However, quick destabilization of HA-CCMs was found in a 10 mM glutathione (GSH) reductive environment (Fig. S4B, ESI†). HA-CCMs revealed decent loading of DTX (Table S1, ESI†). HA-CCMs loaded with 6.6 wt% DTX displayed a narrow distributed size of 85 nm. With the increase of DTX feed ratio to 20%, the micelle size also increased to 94 nm and drug loading efficiency reached saturation. The release of DTX was markedly accelerated by 10 mM GSH (Fig. 1C), signifying the rapid reduction-responsivity of the HA-CCMs. The stability

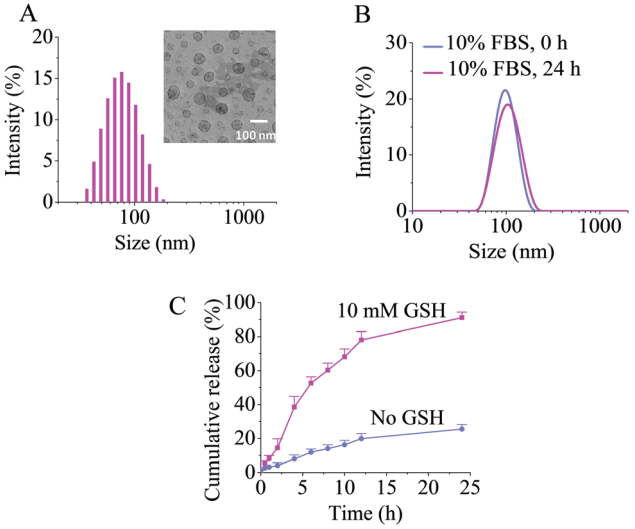

Fig. 1 Size distribution, stability and reduction-sensitivity of HA-CCMs. (A) Size distribution of micelles determined by DLS and size and morphology of micelles obtained by TEM. (B) Micelle stability of HA-CCMs in the presence of 10% FBS. (C) *In vitro* drug release of DTX loaded HA-CCMs either in the presence or absence of 10 mM GSH (pH 7.4, 37 °C).

Table 1 Characterization of HA-CCMs

Entry	DTX feed ratio (wt%)	Size[a] (nm)	PDI[a]	Zeta[b] (mV)	DLE[c] (%)	DLC[c] (wt%)
1	0	80 ± 1	0.07	−27 ± 1	—	—
2	10	85 ± 1	0.11	−26 ± 1	38	4.1
3	15	85 ± 2	0.10	−27 ± 1	40	6.6
4	20	94 ± 2	0.13	−29 ± 2	40	9.1

[a] Determined by dynamic light scattering (DLS), PB (10 mM, pH 7.4). [b] Determined by a Zetasizer Nano-ZS, PB (10 mM, pH 7.4). [c] Drug loading content (DLC) and drug loading efficiency (DLE) determined by HPLC.

of DTX-loaded HA-CCMs in DMEM containing 10% FBS was also studied. Fig. S4C (ESI†) showed that the size of the micelles did not change much in 24 h, indicating that DTX-loaded HA-CCMs are stable in blood.

Targetability and antitumor effect toward CD44-overexpressing MDA-MB-231 cells

MDA-MB-231 breast cancer cells were used as a model to study the targetability of HA-CCMs. To verify their CD44 overexpression, MDA-MB-231 cells were stained with the PE-Cy5 labeled CD44 antibody and observed using confocal and flow cytometry. The results displayed nearly 200-fold stronger fluorescence for MDA-MB-231 cells than for normal fibroblast L929 cells (Fig. S5, ESI† and Fig. 2A), demonstrating high CD44 expression in the MDA-MB-231 cells. To study their cellular uptake, HA-CCMs were labeled with Cy5. Notably, flow cytometry analysis showed the efficient uptake of HA-CCMs by MDA-MB-231 cells in 4 h, which was, nevertheless, significantly prohibited by pretreating the cells with free HA (Fig. 2B), indicating that HA-CCMs are taken up by MDA-MB-231 cells *via* a receptor-mediated pathway.

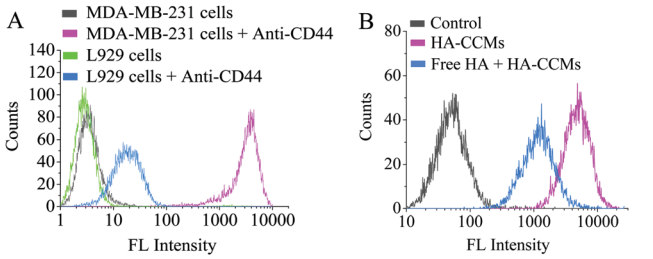

Fig. 2 (A) CD44 receptor expression on MDA-MB-231 breast cancer cells determined by flow cytometry. Normal L929 fibroblast cells were used as the control. (B) Cellular uptake of Cy5-HA-CCMs in MDA-MB-231 breast tumor cells determined by flow cytometry after 4 h incubation. The CD44 receptor blocking experiment was performed by incubating cells with free HA (final concentration: 5 mg mL^{-1}) for 4 h prior to incubation with Cy5-HA-CCMs.

Firstly, the cytotoxicity of blank HA-CCMs was studied by MTT assay in MDA-MB-231 cells, which showed that the blank micelles have good biocompatibility (cell viability >92%, Fig. S6, ESI†). The antitumor effect of DTX-loaded HA-CCMs toward the MDA-MB-231 cells was evaluated by live/dead and apoptosis assays. Fig. 3A shows severe cell shrinkage and death (red) following 4 h of treatment with DTX-loaded HA-CCMs. In addition, the MTT assay also displayed higher cytotoxicity for DTX-loaded HA-CCMs than free DTX, indicating that DTX in HA-CCMs was clearly more potent than free DTX. DTX is known to suppress cell growth by disrupting microtubule assembly and activating the pro-apoptotic signal pathway.[43,44] Apoptosis studies using Annexin V and PI staining confirmed that DTX-loaded HA-CCMs induced significant apoptosis (42%) of the MDA-MB-231 cells, which was slightly more effective than free DTX (36% apoptosis) (Fig. 3B). These results indicate that DTX-loaded HA-CCMs can be efficiently taken up by the

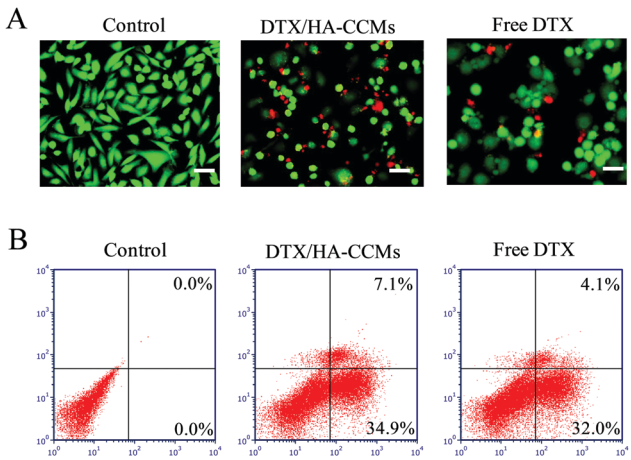

Fig. 3 (A) Live/dead assay of MDA-MB-231 cells after 4 h incubation with either DTX-loaded HA-CCMs or free DTX (1 μg DTX equiv. per mL) and another 44 h culture in fresh medium. Live cells (green) and dead cells (red). Bar: 20 μm. Cells without treatment are used as the control. (B) Apoptosis assay of MDA-MB-231 cells after 4 h incubation with either DTX-loaded HA-CCMs or free DTX (1 μg DTX equiv. per mL) and another 20 h culture in fresh medium. Cells without treatment are used as the control.

MDA-MB-231 cells and that loaded DTX can be rapidly released into the cytoplasm.

Pharmacokinetics, biodistribution and tumor penetration studies

The *in vivo* pharmacokinetic study on tumor-free mice showed that the level of DTX in HA-CCMs firstly quickly decreased due to their distribution from blood to the liver, spleen and other tissues after injection ($t_{1/2\alpha}$ = 0.20 ± 0.04 h), but this $t_{1/2\alpha}$ is still significantly longer ($p < 0.01$) than that of free DTX ($t_{1/2\alpha}$ = 0.01 ± 0.05 h).[45–47] Subsequently, it was noticed that DTX in HA-CCMs had an extended elimination half-time ($t_{1/2\beta}$) of 5.1 h, which was at least 7 times longer than for free DTX ($t_{1/2\beta}$ = 0.72 h, Fig. 4A), demonstrating that HA-CCMs can significantly prolong the circulation time of DTX.[10,17,20] We further studied the tumor accumulation of Cy5-labeled HA-CCMs over time following i.v. injection into MDA-MB-231 breast tumor-bearing mice. As indicated in Fig. 4B, strong tumor accumulation was found at 6–48 h post-injection of Cy5-labeled HA-CCMs, revealing excellent tumor targeting and retention of HA-CCMs in the MDA-MB-231 breast tumor. The tumor accumulation was greatly decreased when mice were pre-treated with free HA, signifying the important role of active targeting in tumor accumulation and retention of HA-CCMs.[48,49] Furthermore, the amount of DTX in the tumor and different organs was quantitatively determined 12 h after injection of DTX-loaded HA-CCMs. Notably, a high tumor accumulation of 6.2% of injected dose per gram of tissue (%ID/g) was observed for DTX-loaded HA-CCMs, which was at least a 4-fold enhancement over free DTX (Fig. 4C).

To investigate their tumor penetration ability, a key factor for tumor therapy,[3,50,51] we examined the distribution of Cy5-labeled HA-CCMs in the MDA-MB-231 tumor 2, 6 and 12 h after injection. The results showed that at 2 h, all HA-CCMs were co-localized with blood vessels (Fig. 5A). At 6 h post injection, Cy5-labeled HA-CCMs were distributed throughout the whole tumor tissue and a prolonged time of 12 h gave even stronger Cy5 fluorescence in the tumor tissue and also inside the

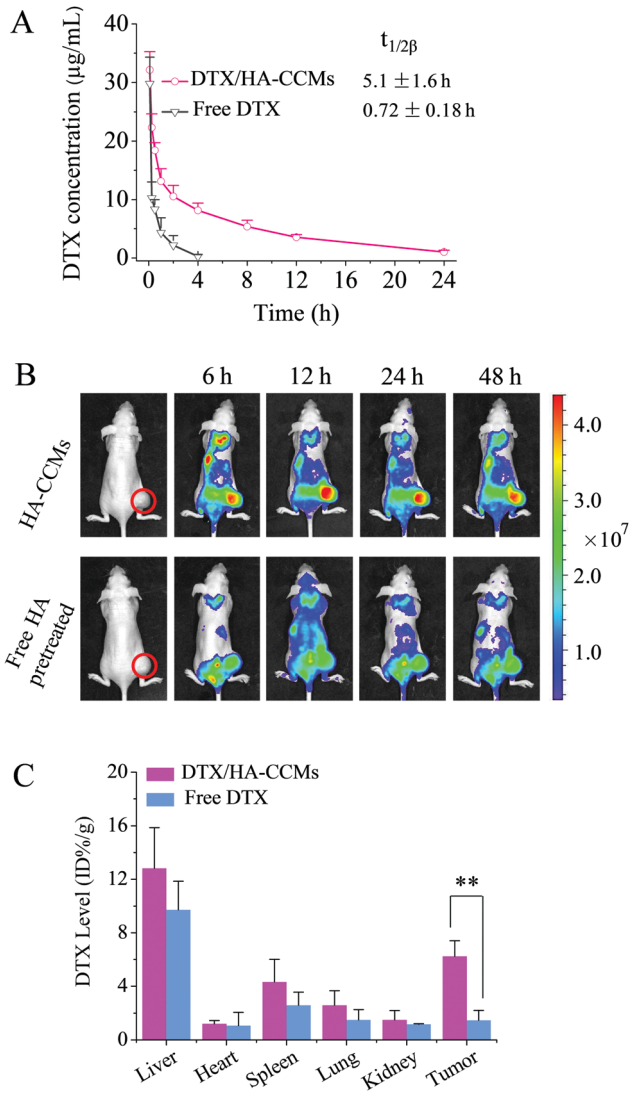

Fig. 4 (A) *In vivo* pharmacokinetics of DTX in HA-CCMs and free DTX in Balb/C mice. (B) *In vivo* imaging of Cy5-labeled HA-CCMs in MDA-MB-231 breast tumor bearing mice. (C) Biodistribution of DTX in the main organs and tumor 12 h after tail vein injection of DTX-loaded HA-CCMs or free DTX (10 mg DTX equiv. per kg).

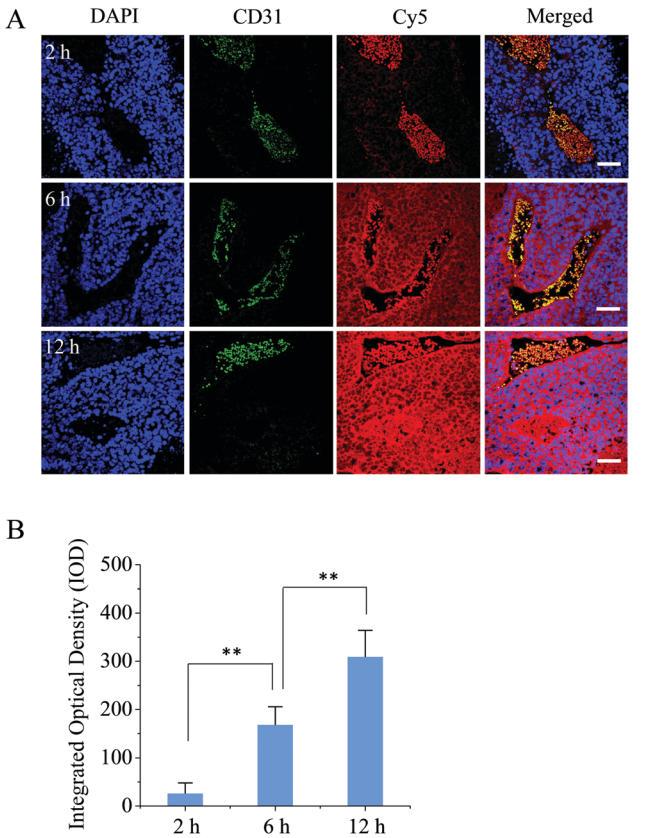

Fig. 5 (A) Tumor penetration behavior of Cy5 labeled HA-CCMs (red) at 2, 6 and 12 h post injection observed using confocal microscopy. Cell nuclei were stained with DAPI (blue). CD31 antibody (green) was used for the staining of tumor blood vessels. The scale bar represents 40 μm. (B) Quantitative analysis for the Cy5 intensity in tumor tissue slices presented as the average integrated optical density (IOD) level at 2, 6 and 12 h. Data are presented as means ± SD (n = 3). **$P < 0.01$.

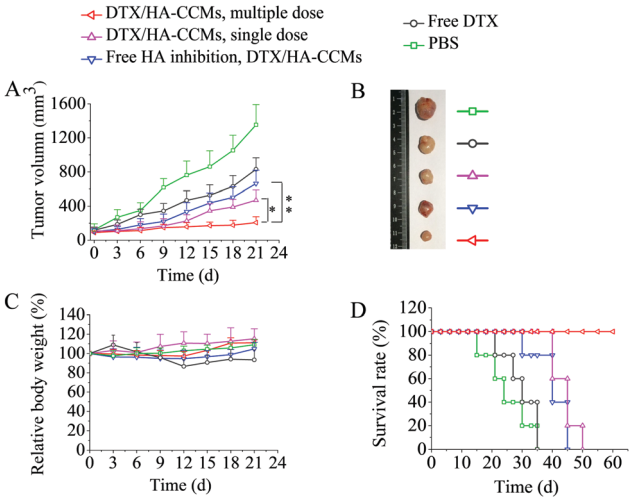

Fig. 6 *In vivo* antitumor efficacy of DTX-loaded HA-CCMs in MDA-MB-231 tumor bearing nude mice with either a single dose or multi-dose treatment. The free DTX, PBS and HA (50 mg kg^{-1}) pre-treated groups were used as controls. The above formulations were intravenously injected into different groups of mice on day 0, 3, 6, 9 and 12 at a dosage of 10 mg DTX equiv. per kg. (A) Tumor growth curves of different mice groups over 21 days, (n = 6). *$p < 0.05$, **$p < 0.01$. (B) Representative tumor blocks removed from mice in different groups at the end of the experiment (day 21). (C) Body weight variations in different groups within 21 days of MDA-MB-231 tumor bearing nude mice. (D) Kaplan–Meier survival curves of nude mice treated with different formulations within 60 days, (n = 5). Data of A and C are given as means ± SD (n = 5).

tumor cells, as indicated by the quantitative analysis for the Cy5 intensity in tumor tissue slices (Fig. 5B). Intratumoral penetration is often a big hurdle for nanomedicines due to the presence of high interstitial fluid pressure (IFP) and dense stromal tissue in the tumor.[52] The long circulation time, efficient tumor accumulation and deep tumor penetration render HA-CCMs particularly interesting for the treatment of MDA-MB-231 breast tumor.

Targeted treatment of MDA-MB-231 human breast tumor

MDA-MB-231 breast tumor-bearing mice were treated with DTX-loaded HA-CCMs in either a single (50 mg DTX equiv. per kg) or a multiple dose scheme (10 mg DTX equiv. per kg, 5 injections). Fig. 6A shows that the multi-dose treatment effectively inhibited tumor growth, which was apparently more effective than the single-dose treatment. In contrast, the multiple injection of free DTX at the same dose could not effectively suppress tumor growth. Moreover, pre-injection of free HA prior to treatment with DTX-loaded HA-CCMs led to a significantly decreased tumor-suppressive effect, signifying the important role of active targeting in MDA-MB-231 cancer treatment. The tumor images corroborated that mice treated with a multi-dose of DTX-loaded HA-CCMs had the smallest tumor volume (Fig. 6B). Fig. 6C displays that only free DTX caused a slight body weight loss and that all micellar formulations were well tolerated. Most remarkably, all mice treated with a multi-dose of DTX-loaded HA-CCMs survived over 60 days (Fig. 6D). In comparison, mice treated with free DTX or PBS all died on day 35. These results point out that DTX-loaded HA-CCMs mediate high-efficiency targeted treatment of CD44-overexpressing MDA-MB-231 breast tumors. The histological analysis using H&E staining showed little damage of normal organs in the micellar DTX treated groups, while obvious cell necrosis was found in the liver of the free DTX treated group (Fig. S7, ESI†). In tumor tissues, mice treated with a multi-dose of DTX-loaded HA-CCMs showed extensive necrosis evidenced by H&E staining and severe apoptosis by TUNEL staining (Fig. 7), which is in line with the superior antitumor efficacy of DTX-loaded HA-CCMs.

Conclusions

We have demonstrated that reduction-responsive, core-crosslinked, and hyaluronic acid-shelled biodegradable micelles (HA-CCMs) mediate the highly potent and targeted chemotherapy of MDA-MB-231 human triple negative breast tumor in nude mice. HA-CCMs fabricated from one single block copolymer possess many interesting properties: (i) they have a decent loading of docetaxel, favorable size, low drug leakage and glutathione-responsive DTX release; (ii) docetaxel-loaded HA-CCMs can selectively target and suppress the growth of MDA-MB-231 cells; (iii) they show a long blood circulation time, strong tumor accumulation and deep tumor penetration; and (iv) docetaxel-loaded HA-CCMs effectively suppress the progression of MDA-MB-231 tumor and significantly improve mice survival time. These simple, selective and bioresponsive micellar systems have

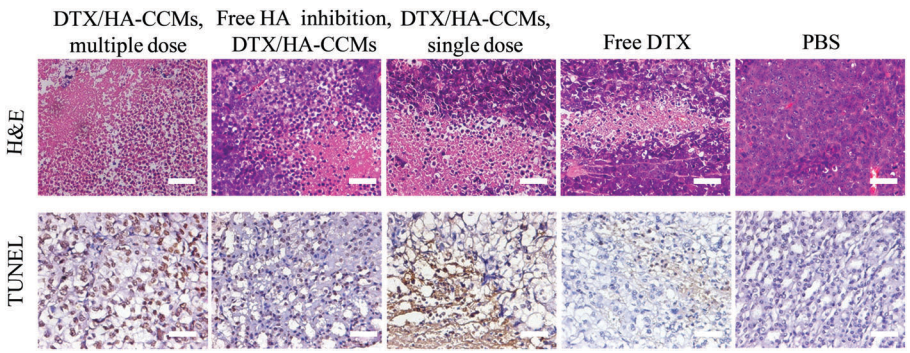

Fig. 7 H&E and TUNEL staining of tumor sections excised from subcutaneous MDA-MB-231 breast tumor bearing nude mice following 21 days of treatment with different formulations (Leica microscope, magnification 400×). Bar: 50 μm.

emerged as a highly appealing platform for targeted chemotherapy of CD44-overexpressing cancers.

Conflicts of interest

There are no conflicts of interest to declare.

Acknowledgements

This work was financially supported by the National Natural Science Foundation of China (51633005, 51773146).

References

1 C. Deng, Y. Jiang, R. Cheng, F. Meng and Z. Zhong, *Nano Today*, 2012, **7**, 467–480.
2 L. Houdaihed, J. C. Evans and C. Allen, *Mol. Pharmaceutics*, 2017, **14**, 2503–2517.
3 J. Shi, P. W. Kantoff, R. Wooster and O. C. Farokhzad, *Nat. Rev. Cancer*, 2017, **17**, 20–37.
4 H. Cabral and K. Kataoka, *J. Controlled Release*, 2014, **190**, 465–476.
5 A. Rösler, G. W. M. Vandermeulen and H.-A. Klok, *Adv. Drug Delivery Rev.*, 2012, **64**, 270–279.
6 R. van der Meel, L. J. Vehmeijer, R. J. Kok, G. Storm and E. V. van Gaal, *Adv. Drug Delivery Rev.*, 2013, **65**, 1284–1298.
7 Y. Zhong, F. Meng, C. Deng and Z. Zhong, *Biomacromolecules*, 2014, **15**, 1955–1969.
8 J. D. Byrne, T. Betancourt and L. Brannon-Peppas, *Adv. Drug Delivery Rev.*, 2008, **60**, 1615–1626.
9 F. Danhier, O. Feron and V. Préat, *J. Controlled Release*, 2010, **148**, 135–146.
10 M. Talelli, M. Barz, C. J. Rijcken, F. Kiessling, W. E. Hennink and T. Lammers, *Nano Today*, 2015, **10**, 93–117.
11 E. Fleige, M. A. Quadir and R. Haag, *Adv. Drug Delivery Rev.*, 2012, **64**, 866–884.
12 H. Yu, Z. Cui, P. Yu, C. Guo, B. Feng, T. Jiang, S. Wang, Q. Yin, D. Zhong, X. Yang, Z. Zhang and Y. Li, *Adv. Funct. Mater.*, 2015, **25**, 2489–2500.
13 J. Li, W. Ke, H. Li, Z. Zha, Y. Han and Z. Ge, *Adv. Healthcare Mater.*, 2015, **4**, 2206–2219.
14 A. Wicki, D. Witzigmann, V. Balasubramanian and J. Huwyler, *J. Controlled Release*, 2015, **200**, 138–157.
15 H. J. Cho, I. S. Yoon, H. Y. Yoon, H. Koo, Y. J. Jin, S. H. Ko, J. S. Shim, K. Kim, I. C. Kwon and D. D. Kim, *Biomaterials*, 2012, **33**, 1190–1200.
16 X. Deng, M. Cao, J. Zhang, K. Hu, Z. Yin, Z. Zhou, X. Xiao, Y. Yang, W. Sheng, Y. Wu and Y. Zeng, *Biomaterials*, 2014, **35**, 4333–4344.
17 Y. Zhong, J. Zhang, R. Cheng, C. Deng, F. Meng, F. Xie and Z. Zhong, *J. Controlled Release*, 2015, **205**, 144–154.
18 X. Han, Z. Li, J. Sun, C. Luo, L. Li, Y. Liu, Y. Du, S. Qiu, X. Ai, C. Wu, H. Lian and Z. He, *J. Controlled Release*, 2015, **197**, 29–40.
19 H. S. S. Qhattal, T. Hye, A. Alali and X. Liu, *ACS Nano*, 2014, **8**, 5423–5440.
20 E. J. Oh, K. Park, K. S. Kim, J. Kim, J. A. Yang, J. H. Kong, M. Y. Lee, A. S. Hoffman and S. K. Hahn, *J. Controlled Release*, 2010, **141**, 2–12.
21 J. Li, M. Huo, J. Wang, J. Zhou, J. M. Mohammad, Y. Zhang, Q. Zhu, A. Y. Waddad and Q. Zhang, *Biomaterials*, 2012, **33**, 2310–2320.
22 Y. Zhu, X. Wang, J. Chen, J. Zhang, F. Meng, C. Deng, R. Cheng, J. Feijen and Z. Zhong, *J. Controlled Release*, 2016, **244**, 229–239.
23 Y. Li, K. Xiao, J. Luo, W. Xiao, J. S. Lee, A. M. Gonik, J. Kato, T. A. Dong and K. S. Lam, *Biomaterials*, 2011, **32**, 6633–6645.
24 Y. Oe, R. J. Christie, M. Naito, S. A. Low, S. Fukushima, K. Toh, Y. Miura, Y. Matsumoto, N. Nishiyama, K. Miyata and K. Kataoka, *Biomaterials*, 2014, **35**, 7887–7895.
25 H. S. Han, K. Y. Choi, H. Ko, J. Jeon, G. Saravanakumar, Y. D. Suh, D. S. Lee and J. H. Park, *J. Controlled Release*, 2015, **200**, 158–166.
26 S. Yu, J. Ding, C. He, Y. Cao, W. Xu and X. Chen, *Adv. Healthcare Mater.*, 2014, **3**, 752–760.
27 Y. Zou, Y. Fang, H. Meng, F. Meng, C. Deng, J. Zhang and Z. Zhong, *J. Controlled Release*, 2016, **244**, 326–335.
28 Y. Zou, F. Meng, C. Deng and Z. Zhong, *J. Controlled Release*, 2016, **239**, 149–158.
29 Y. Zhu, J. Zhang, F. Meng, C. Deng, R. Cheng, J. Feijen and Z. Zhong, *ACS Appl. Mater. Interfaces*, 2017, **9**, 35651–35663.
30 Y. Zou, M. Zheng, W. Yang, F. Meng, K. Miyata, H. J. Kim, K. Kataoka and Z. Zhong, *Adv. Mater.*, 2017, **29**, 1703285.
31 Y. Fang, Y. Jiang, Y. Zou, F. Meng, J. Zhang, C. Deng, H. Sun and Z. Zhong, *Acta Biomater.*, 2017, **50**, 396–406.
32 F. Podo, L. M. C. Buydens, H. Degani, R. Hilhorst, E. Klipp, I. S. Gribbestad, S. Van Huffel, H. W. M. van Laarhoven, J. Luts, D. Monleon, G. J. Postma, N. Schneiderhan-Marra, F. Santoro, H. Wouters, H. G. Russnes, T. Sørlie, E. Tagliabue and A.-L. Børresen-Dale, *Mol. Oncol.*, 2010, **4**, 209–229.
33 G. Bianchini, J. M. Balko, I. A. Mayer, M. E. Sanders and L. Gianni, *Nat. Rev. Clin. Oncol.*, 2016, **13**, 674–690.
34 E. A. Perez, E. H. Romond, V. J. Suman, J. H. Jeong, G. Sledge, C. E. Geyer Jr., S. Martino, P. Rastogi, J. Gralow, S. M. Swain, E. P. Winer, G. Colon-Otero, N. E. Davidson, E. Mamounas, J. A. Zujewski and N. Wolmark, *J. Clin. Oncol.*, 2014, **32**, 3744–3752.
35 J. Cuzick, I. Sestak, S. Cawthorn, H. Hamed, K. Holli, A. Howell and J. F. Forbes, *Lancet Oncol.*, 2015, **16**, 67–75.
36 Y. Fan, Q. Wang, G. Lin, Y. Shi, Z. Gu and T. Ding, *Acta Biomater.*, 2017, **62**, 257–272.
37 Z. J. Deng, S. W. Morton, E. Ben-Akiva, E. C. Dreaden, K. E. Shopsowitz and P. T. Hammond, *ACS Nano*, 2013, **7**, 9571–9584.
38 P. Huang, C. Yang, J. Liu, W. Wang, S. Guo, J. Li, Y. Sun, H. Dong, L. Deng, J. Zhang, J. Liu and A. Dong, *J. Mater. Chem. B*, 2014, **2**, 4021–4033.
39 I. Noh, H. O. Kim, J. Choi, Y. Choi, D. K. Lee, Y. M. Huh and S. Haam, *Biomaterials*, 2015, **53**, 763–774.
40 Y. Zhang, K. Wu, H. Sun, J. Zhang, J. Yuan and Z. Zhong, *ACS Appl. Mater. Interfaces*, 2018, **10**, 1597–1604.

41 B.-P. Jiang, L. Zhang, Y. Zhu, X.-C. Shen, S.-C. Ji, X.-Y. Tan, L. Cheng and H. Liang, *J. Mater. Chem. B*, 2015, **3**, 3767–3776.
42 H. Y. Yoon, H. Koo, K. Y. Choi, I. Chan Kwon, K. Choi, J. H. Park and K. Kim, *Biomaterials*, 2013, **34**, 5273–5280.
43 Y. Luo, Y. Ling, W. Guo, J. Pang, W. Liu, Y. Fang, X. Wen, K. Wei and X. Gao, *J. Controlled Release*, 2010, **147**, 278–288.
44 D. Liu, Z. Liu, L. Wang, C. Zhang and N. Zhang, *Colloids Surf., B*, 2011, **85**, 262–269.
45 K. S. Ho, A. M. Aman, R. S. Al-awar and M. S. Shoichet, *Biomaterials*, 2012, **33**, 2223–2229.
46 S. Jain, N. Bhankur, N. K. Swarnakar and K. Thanki, *Pharm. Res.*, 2015, **32**, 3282–3292.
47 J. Huang, H. Zhang, Y. Yu, Y. Chen, D. Wang, G. Zhang, G. Zhou, J. Liu, Z. Sun, D. Sun, Y. Lu and Y. Zhong, *Biomaterials*, 2014, **35**, 550–566.
48 K. Y. Choi, H. Chung, K. H. Min, H. Y. Yoon, K. Kim, J. H. Park, I. C. Kwon and S. Y. Jeong, *Biomaterials*, 2010, **31**, 106–114.
49 T. Jiang, Z. Zhang, Y. Zhang, H. Lv, J. Zhou, C. Li, L. Hou and Q. Zhang, *Biomaterials*, 2012, **33**, 9246–9258.
50 M. J. Ernsting, M. Murakami, A. Roy and S. D. Li, *J. Controlled Release*, 2013, **172**, 782–794.
51 S. Barua and S. Mitragotri, *Nano Today*, 2014, **9**, 223–243.
52 Q. Sun, T. Ojha, F. Kiessling, T. Lammers and Y. Shi, *Biomacromolecules*, 2017, **18**, 1449–1459.